Innovative Infrastructure Solutions (2023) 8:169
https://doi.org/10.1007/s41062-023-01134-5

TECHNICAL PAPER

Geotechnical behavior of a single pile in sand with varied cross-section geometries and construction techniques

Mohamed A. Sakr[1] · **Waseim R. Azzam**[1] · **Hatem K. Kassim**[1]

Received: 29 July 2021 / Accepted: 26 April 2023 / Published online: 11 May 2023

Abstract

Due to limited investigations that studied the influence of the cross-section geometry on the compression pile resistance, the series of experiments presented in this paper aims to investigate the geotechnical behavior of a single pile in sand with varied the cross-section geometries. In order to achieve this purpose, testing program comprising sex model steel piles with varied cross-section geometries of 20 mm width/diameter was conducted using two construction techniques. The tests are performed on piles with *L*/*D* ratios of 10 and 30 installed in the three cases of sand relative density as medium dense and dense sand. Results indicated that pile cross-section geometry has a significant influence on the compressive capacity. Also, for piles having the same diameter, the closed-ended pipe piles have more resistance comparing with the open-ended and conical base pipe piles at all series conditions, while for non-displacement piles with the same width, the square closed-ended pile is a highly effective compared with the square open-ended and tapered piles. Moreover, for jacked piles with *L*/*D* of 10 and 30, the compressive capacities of tapered piles with *L*/*D* of 10 and 30 in medium dense sand were found to be increased by (9% and 15%) and (15% and 38%) comparing with that of square closed-ended and square open-ended piles, respectively. Furthermore, the results also indicated that the conical base with sixty-degree configuration is the preferred end closure for open-ended pipe piles to provide high performance in the installation process and to achieve load capacity.

Keywords Cross-section geometries · Single pile · Pile installation and sand relative density

List of symbols

D_r	Relative sand density
L/*D*	Pile length to diameter ratio
D	Pile diameter
t	Pile walls thickness
S	Pile settlement
$Q_{max.}$	Maximum loading of pile
$Q_{ult.}$	Ultimate compressive pile capacity
φ	Internal friction angle of sand

✉ Waseim R. Azzam
waseim.azzam@f-eng.tanta.edu.eg

Mohamed A. Sakr
mamsakr@f-eng.tanta.edu.eg

Hatem K. Kassim
PG_90983@f-eng.tanta.edu.eg

[1] Structural Engineering Department, Faculty of Engineering, Tanta University, Tanta, Egypt

Introduction

Piles are commonly used to support offshore platforms, marine structures, tower foundations, bridge abutments and superstructures. Also, the pile capacity and associated settlement play a key role in the design procedures and the construction of pile foundations. Considerable studies were performed in the past to evaluate the pile capacity in sand. Most design approaches and previous studies idealize the pile-soil system to a certain extent. Therefore, the influence of additional factors affecting the pile capacity in sand such as soil characteristics, pile characteristics, methods of pile installation technique, and the nature of loading should be investigated [23, 24]. It is intuitive that the cross-section geometries of pile have a significant influence on the pile resistance. Typically, the full-scale in situ pile tests are performed to evaluate exactly the pile capacities and associated settlement. The large-scale pile tests are being expensive, time-consuming and difficult to perform. Therefore, the small-scale model tests are normally accepted to estimate the pile capacity and reliable alternative to field pile tests to investigate the effects of the base geometry. This paper

introduces previous studies that investigated the effects of the pile cross-section geometry in sand. Existing laboratory-scale studies the effects of the pile cross-section geometry in sand are summarized in Appendix 1. In order to investigate the open-ended pipe piles with limited plugging soil, Fattah and Al-Soudani [14, 15] performed twenty-four model pile tests. The model piles manufactured by closing the pile ends using a welded-plate at distance of 2D, 3D and 4D (where *D*: pile diameter) from the pile tip. From their experiment, it is indicated that the open-ended pipe piles behave as the closed-ended pipe piles in the two cases of partially and fully soil plugged. The results also indicated the soil plug length of 3D has the highest capacity in compression to open-ended pipe pile compared with that of the soil plug length of 2D as well as 4D. On the other hand, Jebur et al. [21] investigated piles in sand using the experimental piles and the ANN approach in three main aspects. These aspects included that the experimental series preformed on three types of model piles of (square concrete, steel open-ended pipe and closed-ended pipe piles) having different slenderness's ratios (12, 17 and 25) to develop the ANN database for model inputs and output parameters. Also, relatively simple model input parameters are required to train the network without the need for in situ tests such as pile-load test (PLT), cone penetration test (CPT) and standard penetration test (SPT). Finally, development of MATLAB code using the Levenberg–Marquardt approach (LM) to the implementation of an ANN model as it is the most reliable method in comparison to all computational intelligence approaches (Jeong and Kim [22]). From the analyzed results, the developed ANN model is highly suited for predicting the load capacity of piles. Also, Salih et al. [36] carried out experiments on the different pile cross sections as closed-ended pipe pile, open-ended pipe pile and H-pile. It is noted that the base area of model piles is the same despite different shapes (78.0 mm^2). The experimental results demonstrated that in the case of loose sand, H-piles have more resistance compared with the closed-ended and open-ended pipe piles at the same experimental properties, while, in the two cases of medium and dense sand, H-piles have less resistance compared with the closed-ended and open-ended pipe piles. Moreover, for the two cases of medium and dense sand, the closed-ended pipe piles have more resistance compared with the open-ended pipe piles under the same experimental properties. Another study on the influence of cross section was conducted by Dario-Tovar et al. [9]. They performed tests in a half-cylindrical test tank that allowed visualization of the sand zone during installation procedure and the loading via the chamber symmetry plane. Also, the digital images that taken during installation and loading were analyzed by digital image correlation (DIC) technique. The results clearly showed that the base geometry of the pile has a significant effect on the mobilized of the unit base resistance. As well as, the displacement and strain fields in the sand around the pile tip is affected by the base geometries of the piles. In addition, the results of DIC technique showed that the sand underneath the tip with a flat base was achieved densification up to 30% compared with that of below piles with a conical base. In addition, Sakr et al. [34] conducted tests on jacked pipe piles with varied cross sections at the pile tip as closed-ended, open-ended and conical base pipe piles. It is noted that the surface area along model piles is the same despite different shapes. Also, the conical base pipe pile consisted of open-ended pipe pile and solid conical cross-sectional base with sixty-degree configuration. As well as, the conical cross-sectional base is made to fit the end of open ended pipe pile. The results showed that the closed-ended pipe pile is the optimum cross section under the same experimental conditions. Moreover, the conical cross-sectional base pipe pile has more resistance compared with open-ended pipe pile for all tests. On the other hand, more investigations studied the effects of the pile shape on the shaft pile resistance for example the family of tapered piles. Manandhar et al. [26] and Manandhar and Yasufuku [27] concluded that a small increase in tapering degree of the pile affects significantly on a higher skin friction compared with conventional straight piles at different sand relative densities.

On the other hand, in the past, White and Deeks [41] reported that the use of pile hammers in urban areas has a negative environmental effect. So, the construction of conventional bored piles is an alternative construction method to reduce the negative environmental effects. In response, high-capacity driving machines have been developed. These developments have been produced to improve the performance of the foundation or to reduce the environmental impact of its construction. Performance is measured by the strength and stiffness of the pile foundations. But, these pile techniques still are environmentally unfriendly technique (Yang et al. [42]). Therefore, there is a need to more advanced approaches or techniques in relation to the pile installation techniques to predict the load–displacement behavior of piles (Salih et al. [36] and Sakr et al. [34]). So, there is a need to select some investigations for example, De Beer [11] introduced the difference behavior of bored and driven piles. This technical report indicated that the base resistance of driven piles increased by about three times compared with the bored piles. Also, Yang et al. [42] described field investigation to study the differences and similarities between jacked and driven H-piles in silty sand. The field results clearly showed that the shaft resistances of the jacked piles have higher stiffness and strength compared with driven piles. However, driven piles have higher base resistance compared with the jacked piles. Additionally, Adejumo [1] conducted laboratory and field investigations on model cylindrical, square and tapered piles. The piles were installed by driving and boring methods. From

the results, it is concluded that the capacities of tapered piles were 1.5–2 times larger than the capacities of square piles; and 2–3 larger than the capacities of cylindrical piles. Also, piles installed by driving methods (hammer /or vibration) have more resistance compared with piles installed by boring methods. On the other hand, Basu and Prezzi [6] described the behavior of piles depending on the nature of their displacement for example, during the installation of the full-displacement piles, significant changes in the void ratio and stress state of the in situ soil occur because the soil surrounding the pile's walls is mainly displaced in the lateral direction as well as the soil below the pile tip is preloaded. These changes produce a stiffer load–displacement response for the displacement piles compared with the non-displacement piles, particularly in the case of sand which gain additional strength through densification. Also, there are other types of piles as H-piles, some auger piles and open-ended pipe piles that demonstrated behavior intermediate between non-displacement and full-displacement piles. These piles are often called partial-displacement piles.

From the literature review, it can be clearly observed that there is a lack of data concerning the influence of the pile cross-section geometry on pile resistance. Moreover, the design approaches used in practice for full-displacement, partial-displacement and non-displacement piles in sand are not considering these effects on the pile compression capacity calculations. Therefore, this research aimed to investigate the geotechnical behavior of a single pile in sand with varying the cross-section geometry by conducting experiments on sex model steel piles with varied cross-section geometries. Furthermore, this experimental work provides a comprehensive study through performing static compressive load tests on different model piles with two different lengths installed in sand with two different relative densities, as well as two construction techniques. It should be noted that in this current study, the results and comparisons between the piles that have the same shaft surface area, whether circular or square in shape, will be analyzed separately in order for the comparisons to be fair.

Experimental work

Test tank

The pile load tests were performed in steel test tank with internal dimensions of 800 × 800 mm in plan and 800 mm in height. The wall thickness of test tank is 4 mm to avoid any lateral deformation of the side walls. Test tank is connected directly with two steel columns using a special guide. These columns are firmly fixed in two horizontal steel beams, which are firmly stabled in the lab ground. In this present study, the internal dimensions of test tank were chosen so as to minimize the boundary effect between soil grains and sides of the test tank. According to the related literature, the distance between the pile elements and the walls of test tank should be in excess of 10 times pile diameters as proposed by Phillips and Valsangkar [31] and Bolton et al. [8]. Furthermore, Garnier et al. [16] recommended that the ratio between the width of test tank and the pile diameter should be in excess of 35. In this present study, the distance between the pile elements and the walls of test tank is equal to 390 mm = 19.5D. Also, the ratio between the width of test tank and the pile diameter is equal to 40. Therefore, the inner dimensions of test tank were taken so as according to the recommended ratios.

Axial compression loads on different model piles were applied gradually in small increments using a hand operated hydraulic jack. The loads were measured using load cell to record the applied compression load. Steel plates were located centrally on the width of test tank to support base of magnetic bars for two dial gauges as shown in Fig. 1. Two dial gauges were placed at equal distances from the pile axis. The readings of dial gauge were recorded form both dial gauges for each increment of compression loading when it becomes stable. The axial displacement of the pile corresponding to the applied axial compression load has been taken as the average value of displacement that were recorded from both dial gauges. The experimental set up is shown in Fig. 1. During pile driving or pile loading, the soil surrounding the pile will be disturbed. The disturbed area depended on both of pile installation method and soil relative density. Based on that, Robinsky and Morrison [33] recommended that the disturbed area underneath the pile base should be within the range of 3D-8D from the pile tip, where D: pile diameter. In this experimental work, the distance between from pile to the edge of test tank is ranged from 10 to 30D that is in excess of the recommended ratio.

Sand used

The tests were performed on dry, commercially available sand at Tanta city/Egypt (longitude 31° 00′ 04" E, and latitude 30° 78′ 65" N). The sand used in this study is classified as poorly graded (SP) according to the Unified Soil Classification System (ASTM). Specifications were performed in order to classify the sand used. Physical properties of the used sand are summarized in Table 1. The sand used has round particles that helped in minimizing the resistance between the test tank walls and soil. To maintain the influence of grain size distribution on the combined pile-soil interaction; Balachowski [5] proposed that the ratio between the proposed model pile diameters (D) to the mean grain size diameter (d_{50}) of the sand used must be in excess of 35 for vertical loading. In this model study, (D/d_{50}) ratio is equal to 35.71 that is sufficient.

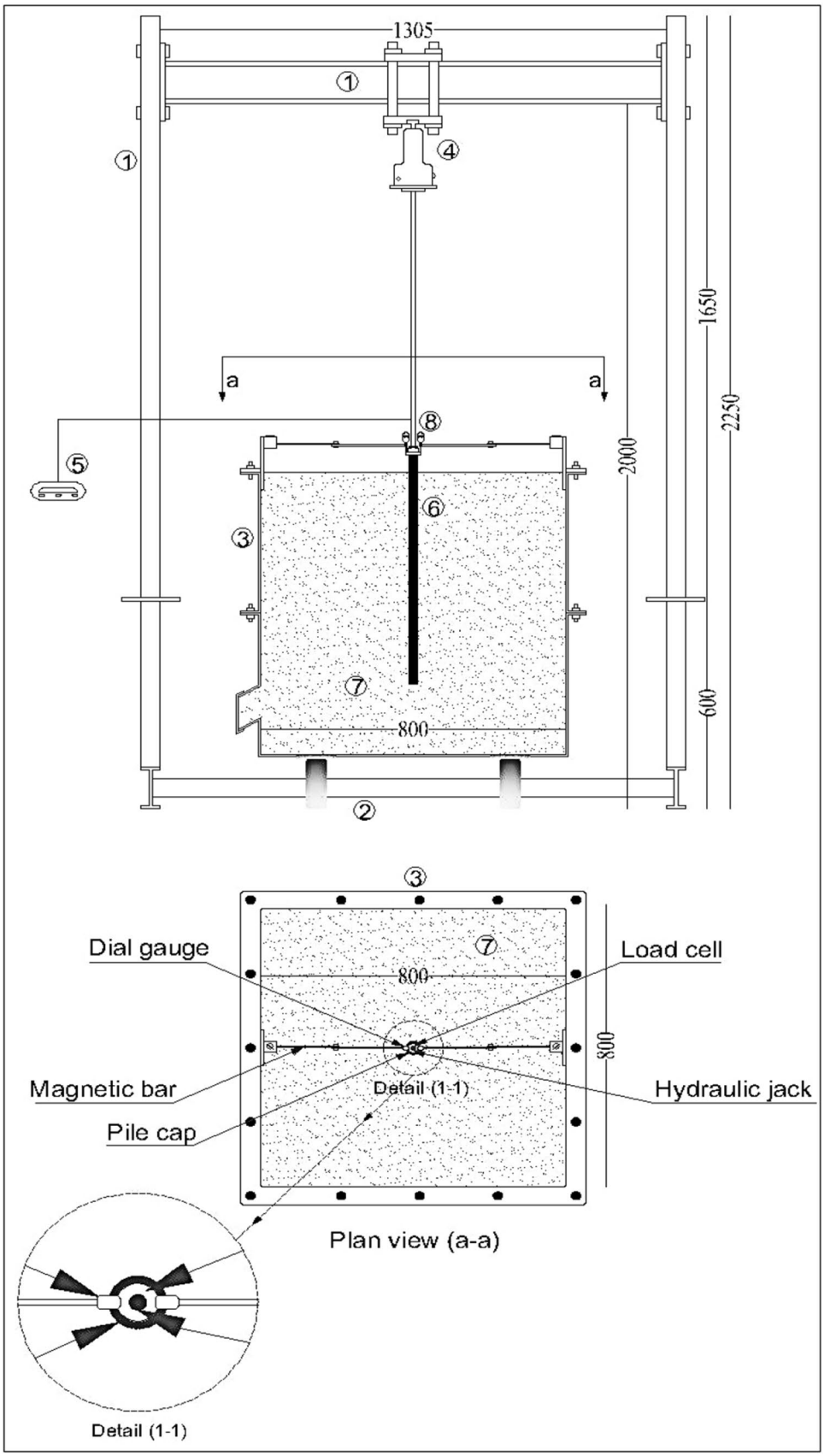

Fig. 1 The experimental set up. (1) Loading frame, (2) Base of loading frame, (3) Test tank, (4) Hydraulic jack, (5) Load cell, (6) Model pile, (7) Sand and (8) Dial gauges

Table 1 Physical properties of the used sand

Properties	Value
Maximum unit weight, $\gamma_{max.}$ (kN/m^3)	19.14
O.M.C (%)	8.11
Minimum unit weight, $\gamma_{min.}$ (kN/m^3)	14.88
Specific gravity (G_s)	2.66
The effective grain size, D_{10} (mm)	0.22
D_{30} (mm)	0.39
Mean grain size, D_{50} (mm)	0.56
D_{60} (mm)	0.66
Uniformity coefficient, C_u	3
Coefficient of curvature, C_c	1.05
Classification, USCS	SP
Maximum void ratio, e_{max}	0.45
Minimum void ratio, e_{min}	0.39
Modeling sand properties	
Dense sand	
Unit weight, γ_{dense} (kN/m^3)	18.11
Relative density, D_r (%)	80
Internal friction angle, φ (degree)	40.1
Medium dense sand	
Unit weight, $\gamma_{medium\ dense}$ (kN/m^3)	17.17
Relative density, D_r (%)	60
Internal friction angle, φ (degree)	36.9

For conducting the experiments, sand was placed in layers, with each layer having 50 mm thick. To prepare the sand with a given relative density, the predetermined weight method was used Salih et al. [36] and Rahil et al. [32]. The relative densities chosen were modeled as medium dense sand ($D_r = 60\%$) and dense sand ($D_r = 80\%$). The relative sand density achieved during the sand preparation was monitored by collecting samples in small cans of known volume placed at different locations in test tank at the time of filling and sand density determined as Nazir and Nasr [29]. The relative sand densities obtained using cans were found to be within the range of $D_r = 60\% \pm 1.22\%$ for the medium dense sand state and $D_r = 80\% \pm 1.37\%$ for the dense sand state.

Model piles

Sex different piles of open-ended pipe, closed-ended pipe and conical cross-sectional base pipe, square open-ended, square closed-ended and tapered with 20 mm diameter/width are used as tested models as shown in Fig. 2. The pile penetration depths were taken as 200 and 600 mm. The pile length-to-diameter (L/D) ratios were taken as 10 and 30, respectively. It should be noted that the pile walls thickness (t) was 1.3 mm giving (D/t) ratio equal to 15.38 within the range of (15–45) for the open-ended pipe piles as suggested by Jardine and Chow [20]. Furthermore, steel conical base has a sixty-degree configuration to close open-ended pipe piles. Finally, tapered piles (prismatic square) are consisted of a difference in axial width at their top and bottom along the length of model pile. Geometry configuration of model piles is shown in Table 2.

Installation procedures of model pile

Figure 3 shows the two different methods of pile installation. For jacking technique, sand was prepared inside test tank; then, model pile was located vertically on the top of sand using a special guide; finally, model pile was installed in sand using a hydraulic compression jack to the desired depth as shown in Fig. 3a, while, for non-displacement technique, model pile was placed vertically to the desired depth using a special guide; then sand was prepared into test tank as shown in Fig. 3b.

Testing program

After the model test preparation is completed, the loading test was performed (singular since 1 pile = 1 test) as shown in Fig. 1. The test was run following the procedure as recommended by Dharmatti and Rakaraddi [12]. The load was applied incrementally until the vertical settlement exceeded 25% of the used pile diameter or reaching failure. A total of 48 experiments were conducted. Table 3 summarizes the testing program.

Results and discussion

Definition of failure load

The ultimate axial capacities of model piles were estimated from load- settlement curves. The settlement is normalized against pile diameter in non-dimensional. Terzaghi [37] and Meyerhof [28] proposed that the ultimate axial pile capacities are estimated from the load–displacement curve as the load corresponding to displacement of 10% D. Additionally, Das [10] described that the end-bearing resistance is in fact mobilized within few percent of pile settlement. In this present study, the ultimate pile capacity ($Q_{ult.}$) is derived from 10% D settlement for load-settlement curves.

Load–displacement relationship

From these tests, the load–displacement curves were obtained and are presented in Figs. 4, 5, 6 and 7).

Figure 4a indicates the relationship of the compression load versus settlement curves for different non-displacement piles having $L/D = 10$ in medium dense sand ($D_r = 60\%$).

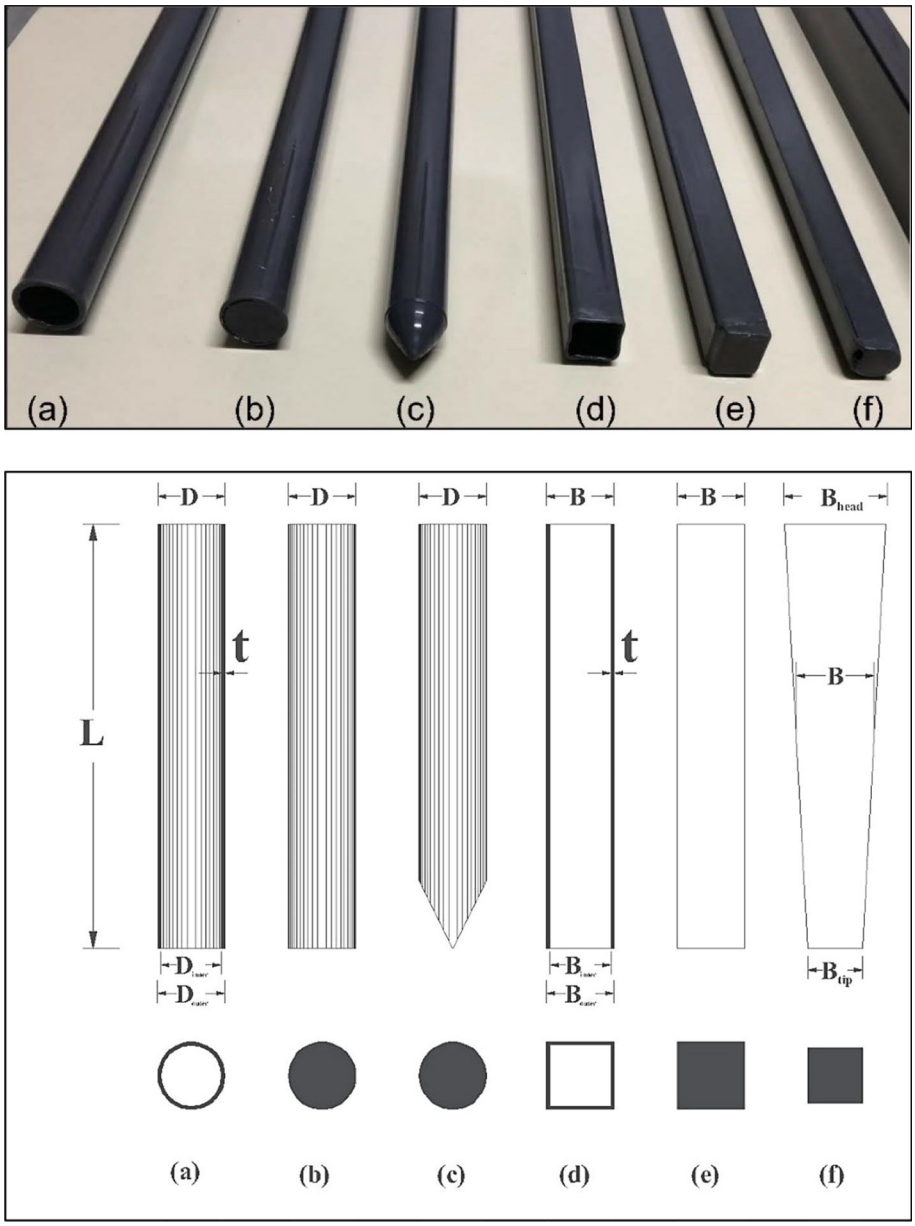

a. Open-ended pipe pile (OEPP)
b. Closed-ended pipe pile (CEPP)
c. Conical base pipe pile (CBPP)
d. Square open-ended pile (SOEP)
e. Square closed-ended pile (SCEP)
f. Tapered pile (TP)

D: pile diameter; D_{inner}: inner pile diameter; D_{outer}: outer pile diameter; B: pile width; B_{inner}: inner pile width; B_{outer}: outer pile width; B_{head}: width of head pile; B_{tip}: width of tip pile; L: pile length and t: pile wall thickness

Fig. 2 Model piles with varied cross sections. D: pile diameter; Dinner: inner pile diameter; Douter: outer pile diameter; B: pile width; Binner: inner pile width; Bouter: outer pile width; Bhead: width of head pile; Btip: width of tip pile; L: pile length and t: pile wall thickness

Table 2 Geometry configuration of model piles

Model piles	A_b (mm^2)	A_s (mm^2)		D or B (mm)			L/D	α (°)
		L = 200 (mm)	L = 600 (mm)	Pile head	Avg	Pile tip		
Open-ended pipe pile (OEPP)	76.37	12,476	37,428		20		10 and 30	0
Closed-ended pipe pile (CEPP)	314.16	12,476	37,428		20			0
Conical base pipe pile (CBPP)	628.32	12,476	37,428		20			0
Square open-ended pile (SOEP)	97.24	16,000	48,000		20			0
Square closed-ended pile (SCEP)	400	16,000	48,000		20			0
Tapered pile (TP)	225	16,000	48,000	25	20	15		1.43 and 0.48

A_b: pile base area; A_s: Surface area of the pile; D: pile diameter; B: pile width; L/D: pile length-to-diameter ratio and α: tapering degree of pile

This figure indicates that the punching failure occurred for open-ended pipe pile up to the maximum ($Q_{max.}$) value approximately equal to 115N corresponding to the displacement of about 22% D. The observed ($Q_{ult.}$) results were found to be 216N, 103N, 115N, 191N, 137N and 164N for closed-ended pipe, open-ended pipe, conical base pipe, square closed-ended, square open-ended and tapered piles, respectively.

Moreover, Fig. 4b indicates load-settlement curves for different non-displacement piles with $L/D = 30$ in medium dense sand ($D_r = 60\%$). This figure indicates that for open-ended pipe, square open-ended, and tapered piles nonlinear relationship until the displacement of approximately 10% D; afterward, it is linear. The same figure also indicates that; the punching failure occurred for open-ended pipe and conical base pipe piles until the maximum ($Q_{max.}$) values approximately equal to 141N and 146N, respectively, corresponding to the displacement of about 11% and 12% D, respectively. The corresponding capacities ($Q_{ult.}$) were found to be 321N, 141N, 146N, 341N, 185N and 280N for closed-ended pipe, open-ended pipe, conical base pipe, square closed-ended, square open-ended and tapered piles, respectively. It can be concluded that the piles installed in medium dense sand have more resistance than piles installed in loose sand. This observation is due to that the friction angle of sand (φ) has a great influence on the shaft resistance of pile (Q_s). It has been clearly observed that the relative sand density has a major influence on the axial pile load capacity.

Furthermore, Fig. 5a indicates load-settlement curves for different jacked piles with $L/D = 10$ in medium dense sand ($D_r = 60\%$). It is observed that for open-ended pipe, conical base pipe, square open-ended, closed-ended pipe and tapered piles, nonlinear relationship until the displacement of almost 10% D; afterward, it is linear. It is also indicated that for square closed-ended and piles nonlinear relationship until the displacement of almost 5% D; afterward, it is linear. The same figure also showed that the punching failure occurred for open-ended pipe and conical base pipe piles until the maximum ($Q_{max.}$) values approximately equal to 386N and 465N, respectively, corresponding to the displacement of about 12 and 30% D, respectively. The observed capacities ($Q_{ult.}$) were found to be 553N, 385N, 439N, 518N, 493N and 566N for closed-ended pipe, open-ended pipe, conical base pipe, square closed-ended, square open-ended and tapered piles, respectively.

Additionally, Fig. 5b indicates load-settlement curves for different jacked piles with $L/D = 30$ in medium dense sand ($D_r = 60\%$). It is observed that for model piles, nonlinear relationship until the displacement of almost 10% D; afterward, it is linear. It also observed that the punching failure occurred for open-ended pipe and conical base pipe piles until the maximum ($Q_{max.}$) values approximately equal to 457N and 489N, respectively, corresponding to the displacement of about 15% and 12% D, respectively. The corresponding ultimate capacities ($Q_{ult.}$) were found to be 678N, 453N, 486N, 610N, 510N and 704N for closed-ended pipe, open-ended pipe, conical base pipe, square closed-ended, square open-ended and tapered piles, respectively.

There is a highly interesting observation obtained from the analyzed results in Figs. 4 and 5, it is found that open-ended and conical base pipe piles using jacking technique showed punching failure later than that of non-displacement piles. This observation is due to sand particle crushing along pile wall and sharp edges of the pile base during the installation of jacking technique as described by Tovar-Valencia et al. [38] and Yuan et al. [43]. Therefore, the soil densification occurred underneath the pile tip.

Figure 6a illustrations load-settlement curves for different non-displacement piles with $L/D = 10$ in dense sand ($D_r = 80\%$). It is clear that for model piles, nonlinear relationship until the displacement of about 10% D; afterward, it is linear. At the displacement of about 10% D, the corresponding ultimate capacities ($Q_{ult.}$) were found to be 240N, 172N, 153N, 220N, 194N and 211Nfor closed-ended pipe, open-ended pipe, conical base pipe, square closed-ended, square open-ended and tapered piles, respectively. The same figure also shows that; the ($Q_{ult.}$) value of open-ended pipe pile was found to be increased by 13% compared with that of conical base pipe pile. In contrast, conical cross-sectional base pipe pile has more resistance than

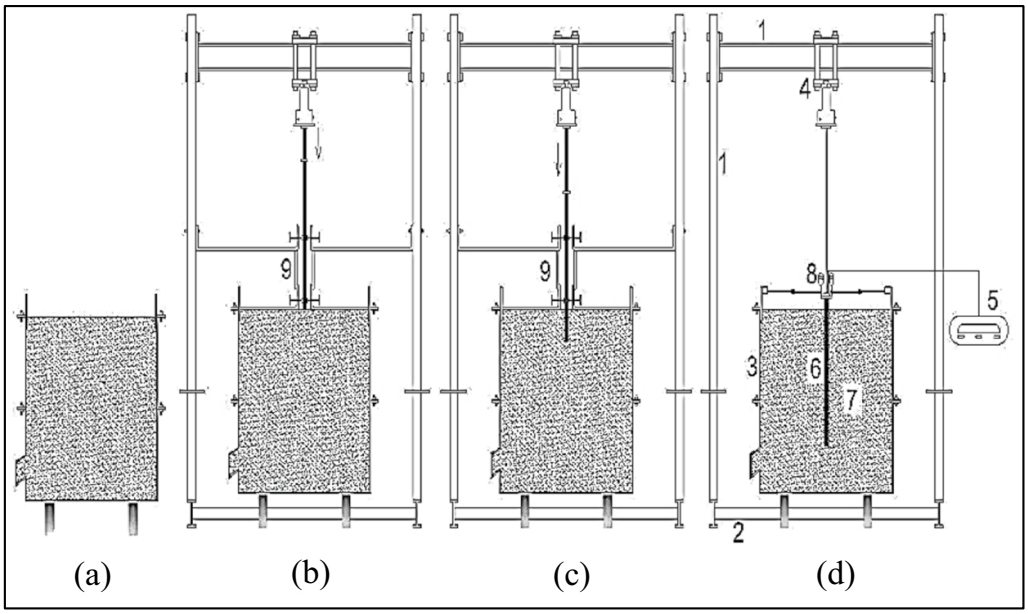

a) Jacking technique

a. Preparing sand inside the test tank

b. Placing model pile vertically on the top of sand using a special guide

c. Installing model pile in sand using a hydraulic jack

d. Completing experimental setup before testing

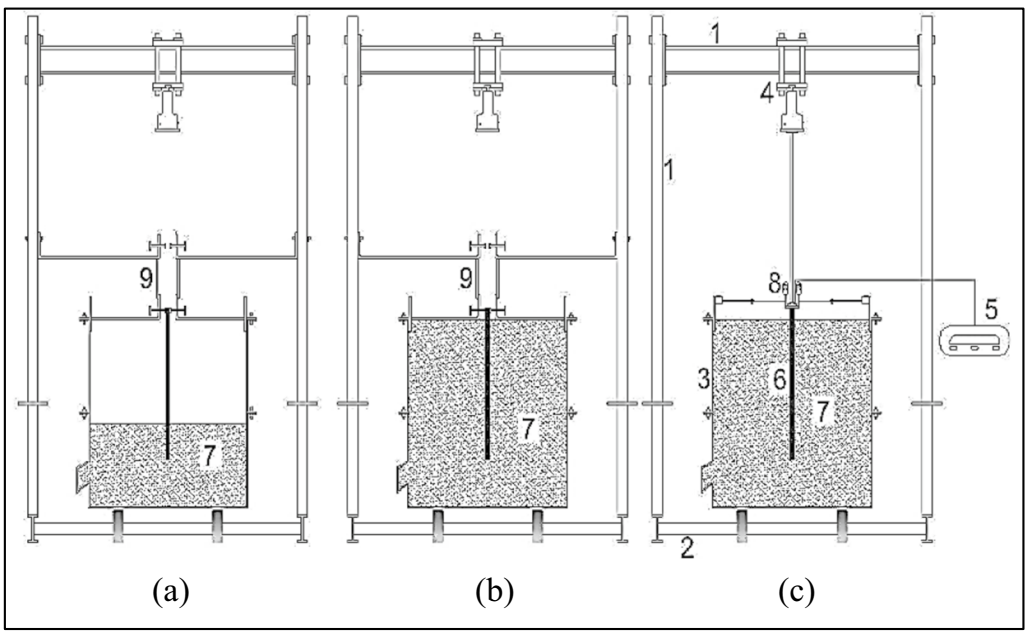

b) Non-displacement technique

a. Placing model pile vertically to the desired depth using a special guide

b. Preparing sand inside the test tank

c. Completing experimental setup before testing

◂**Fig. 3** Installation procedures of model pile. (1) Loading frame, (2) Base of loading frame, (3) Test tank, (4) Hydraulic jack, (5) Load cell, (6) Model pile,(7) Sand, (8) Dial gauges and (9) Special guide

open-ended pipe pile at the same conditions in the case of medium sand. This observation may be due to the effect of soil plugging for open-ended piles increases with the increases of sand relative density.

On the other hand, Fig. 6b indicates load-settlement curves for different non-displacement piles with $L/D = 30$ in dense sand ($D_r = 80\%$). This figure indicates that for model piles, nonlinear relationship until the displacement of almost 10% D; afterward, it is linear. The same figure also indicates that; the corresponding capacities ($Q_{ult.}$) were found to be 425N, 259N, 172N, 475N, 312N and 399N for closed-ended pipe, open-ended pipe, conical base pipe, square closed-ended, square open-ended and tapered piles, respectively.

Furthermore, Fig. 7a indicates load-settlement curves for different jacked piles with $L/D = 10$ in dense sand ($D_r = 80\%$). It is observed that for model piles, nonlinear relationship until the displacement of almost 10% D; afterward, it is linearly. The corresponding capacities ($Q_{ult.}$) were found to be 637N, 425N, 494N, 594N, 542N and 670N for closed-ended pipe, open-ended pipe, conical base pipe, square closed-ended, square open-ended and tapered piles, respectively.

Finally, Fig. 7b indicates load-settlement curves for different jacked piles with $L/D = 30$ in dense sand ($D_r = 80\%$). It is observed that for open-ended pipe, square open-ended, square closed-ended and conical base pipe piles, nonlinear relationship until the displacement of about 10% D; afterward, it is linear. It is also observed that for closed-ended pipe and tapered piles, nonlinear relationship until the displacement of almost 5% D; afterward, it is linear. The corresponding ultimate capacities ($Q_{ult.}$) were found to be 1035N, 698N, 954N, 812N, 746N and 1111N for closed-ended pipe, open-ended pipe, conical base pipe, square closed-ended, square open-ended and tapered piles, respectively.

It should be noted that the vertical displacement readings of a two dial gauge were nearly identical during the pile load test for conical base pipe pile. This observation is due to the advantage of conical base that distributes the driven load evenly around the pile circumference and not causing added stresses on one section of the pile as described by Erhart [13]. In this model study, conical base pipe piles are used as a modified alternative to open-ended pipe piles to install piles into hard layer (dense sand, $D_r = 80\%$) using jacking technique. The results showed that conical cross-sectional base pipe pile has more resistance than open-ended pipe pile. Also, API [2, 3] recommended that the conical cross-sectional base pipe pile should be designed and checked to ensure that it does not decrease the base load capacity of the plugging soil lower than the estimated value in the design. Therefore, according to the estimated methods of the compressive pile capacity, the conical cross-sectional base pipe pile has still more resistance than open-ended pipe pile due to larger surface area, while more investigations described that the load capacity of open-ended pipe piles increase with increasing the pile diameters due to the influence of soil plugging.

Influence of pile cross section

To study the influence of the pile cross section on its axial capacity, sex different piles with the same geometry properties are used as tested models. The relation between axial

Table 3 Testing program

Group	Series	Model pile condition	Variable parameters		No. of tests
			Jacking technique	Non-displacement technique	
Group (1): medium dense sand, $D_r = 60\%$	S_1	Open-ended pipe pile	(L/D) ratio = 10 and 30		4
	S_2	Closed-ended pipe pile			4
	S_3	Conical base pipe pile			4
	S_4	Square open-ended pile			4
	S_5	Square closed-ended pile			4
	S_6	Tapered pile			4
Group (2): dense sand, $D_r = 80\%$	S_7	Open-ended pipe pile	(L/D) ratio = 10 and 30		4
	S_8	Closed-ended pipe pile			4
	S_9	Conical base pipe pile			4
	S_{10}	Square open-ended pile			4
	S_{11}	Square closed-ended pile			4
	S_{12}	Tapered pile			4
Total number of tests					48

D_r: relative sand density and L/D: pile length to diameter ratio

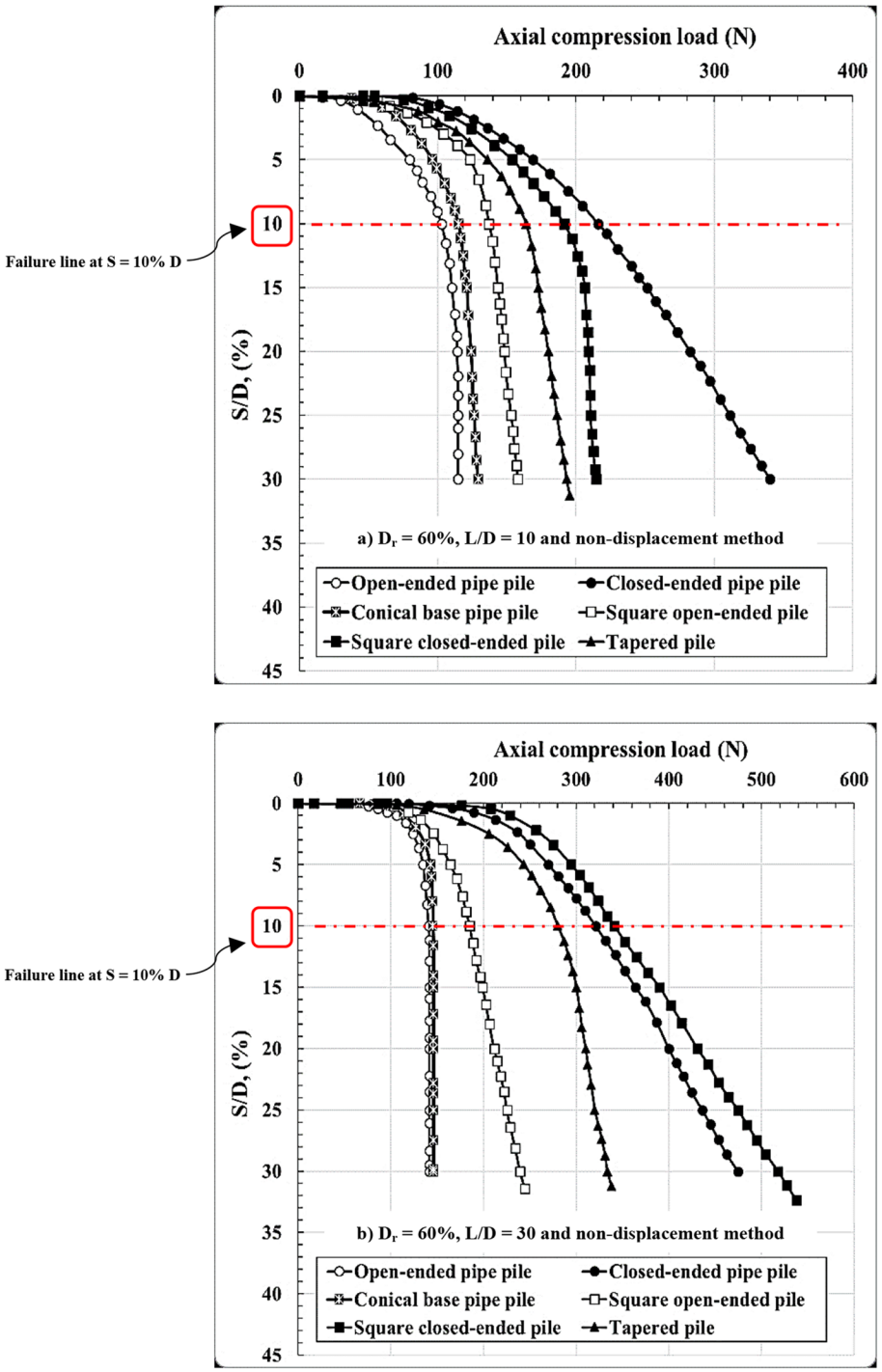

Fig. 4 Load-settlement curves for different non-displacement piles in medium dense sand

compression load and settlement for the six model piles are shown in Figs. 4, 5, 6 and 7. The difference in axial pile capacities is referred to the change in the end bearing stress at the pile tip due to the different pile configurations which have different cross-sectional area. And also, the radial stress around the pile perimeter due to the different pile cross sections that have a great influence in the earth pressure that highly affected on pile capacity. From the analyzed results, it should be noted that the geometry of pile cross section has a significant influence on the pile capacity.

Non-displacement piles

The summary of the compressive capacities for non-displacement piles is presented in Table 4. For piles having

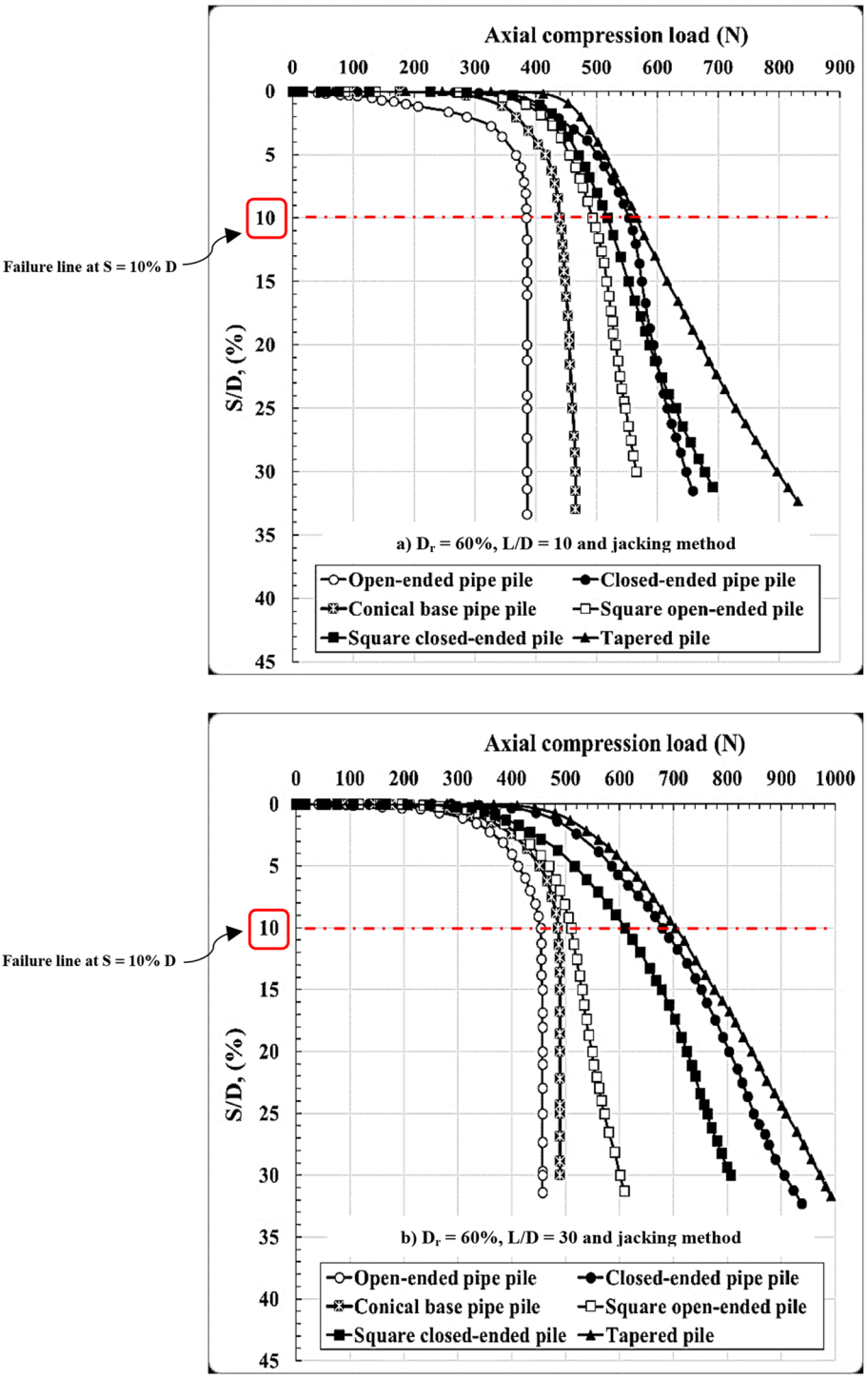

Fig. 5 Load-settlement curves for different jacked piles in medium dense sand

the same diameter, for the two cases of $L/D = 10$ and 30, the ultimate capacities ($Q_{ult.}$) of closed-ended pipe piles were found to be increased by (110% and 128%) and (39% and 64%) compared with that of open-ended pipe piles in the two cases of medium dense and dense sand, respectively. Moreover, for piles with L/D ratio of 10 and 30, the ultimate capacities ($Q_{ult.}$) of closed-ended pipe piles were found to be increased by (87% and 121%) and (57% and 147%) compared with that of conical base pipe piles in the two cases of medium dense and dense sand, respectively. Comparing among piles having the same diameter; it is found that the closed-ended pipe piles have more resistance compared with the open-ended pipe [36] and conical base pipe piles.

On the other hand, for piles having the same width in medium dense sand, for the two cases of $L/D = 10$ and 30,

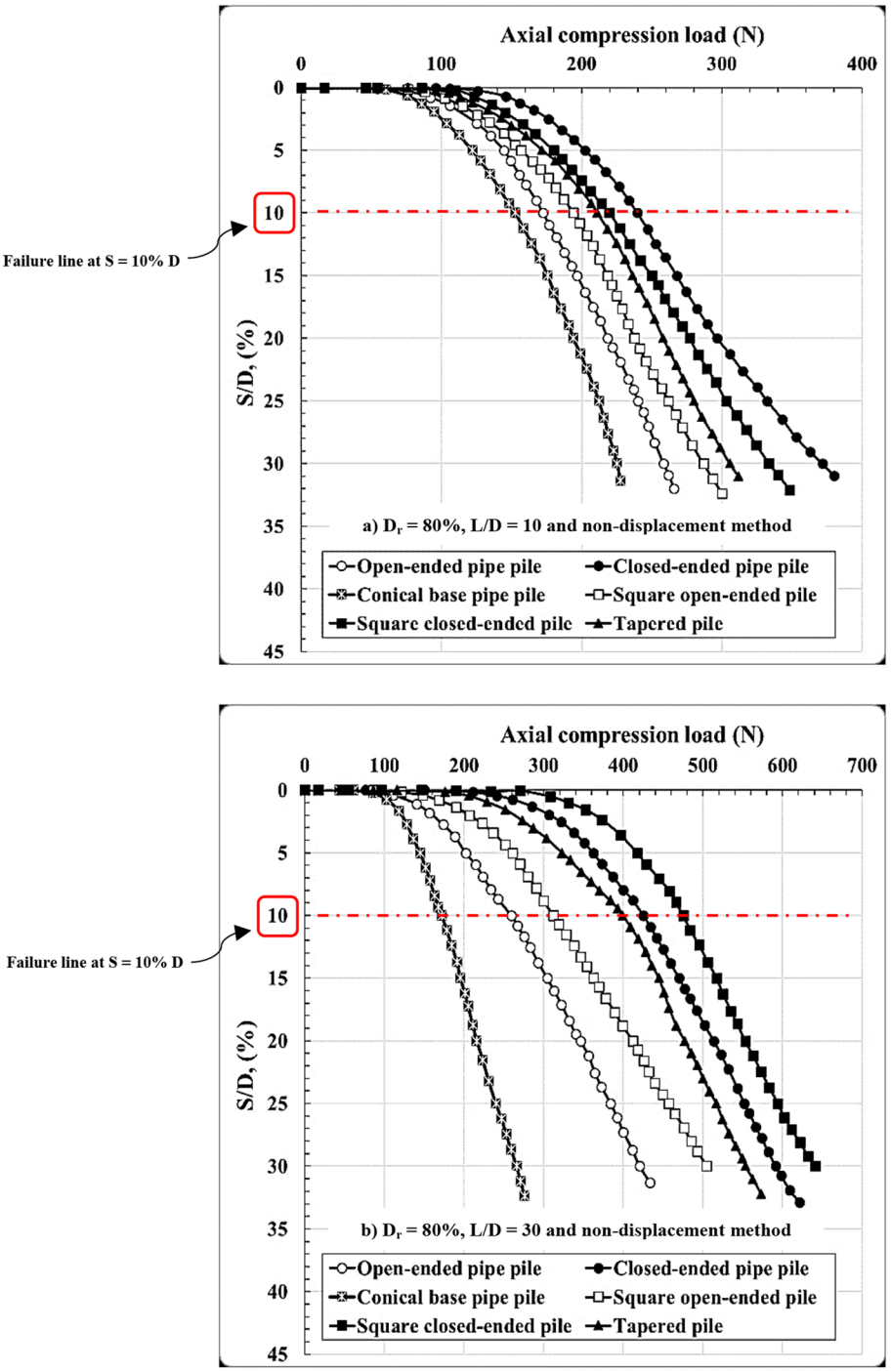

Fig. 6 Load-settlement curves for different non-displacement piles in dense sand

the ultimate capacities ($Q_{ult.}$) of square closed-ended piles were found to be increased by (40% and 17%) and (84% and 22%) compared with that of square open-ended and tapered piles, respectively, while these values were found to be increased by (13% and 4%) and (52% and 19%) in the case of dense sand. Comparing among non-displacement piles with the same width; it is found that the square closed-ended pile is a highly effective and more resistance compared with the square open-ended [19] and tapered piles. This observation is due to square closed-ended piles have a large cross-sectional area.

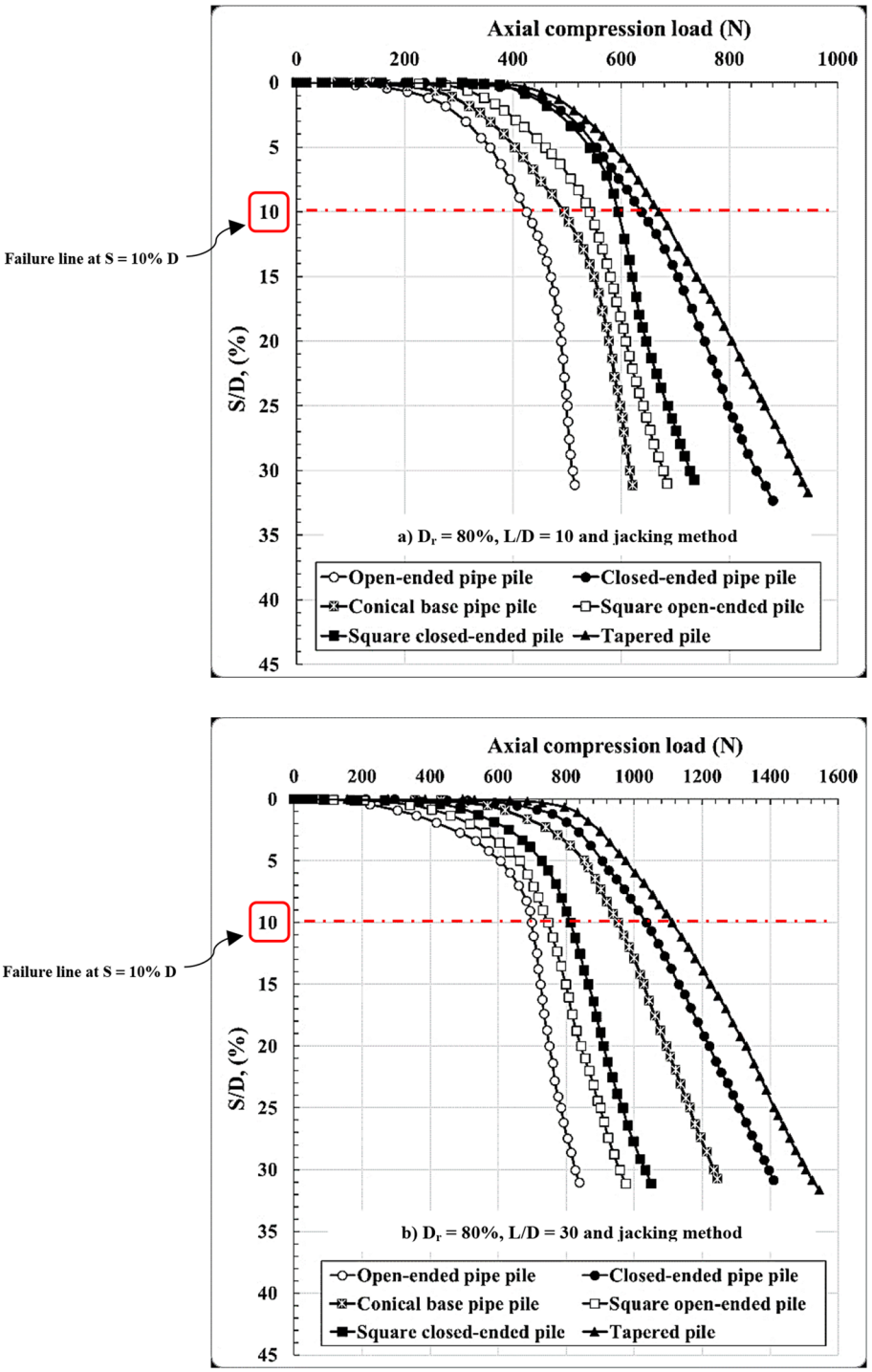

Fig. 7 Load-settlement curves for different jacked piles in dense sand

Jacked piles

The summary of the ultimate compressive capacities for jacked piles is presented in Table 5. For piles having the same diameter, for the two cases of $L/D = 10$ and 30, the ultimate capacities ($Q_{ult.}$) of closed-ended pipe piles were found to be increased by (44% and 50%) and (50% and 48%) compared with that of open-ended pipe piles in the cases of medium dense and dense sand, respectively. From the same table, for piles with L/D of 10 and 30, the ultimate capacities ($Q_{ult.}$) of closed-ended pipe piles were found to be increased by (26% and 40%) and (29% and 8%) compared with that of conical base pipe piles in the cases of medium dense and dense sand, respectively. Also, for piles with L/D of 10 and 30, the ultimate capacities ($Q_{ult.}$) of conical base pipe piles were found to be increased by (14% and 7%) and (16% and

Table 4 The ultimate compressive capacities of non-displacement piles

Relative density	Ultimate compressive capacity, $Q_{ult.}$ (N)											
	Pile length to diameter (L/D) ratio = 10						Ultimate compressive capacity, $Q_{ult.}$ (N)					
	CEPP	OEPP	CBPP	SCEP	SOEP	TP	CEPP	OEPP	CBPP	SCEP	SOEP	TP
Medium dense sand $D_r = 60\%$	216	103	115	191	137	164	321	141	146	341	185	280
Dense sand $D_r = 80\%$	240	172	153	220	194	211	425	259	172	475	312	399

CEPP: closed-ended pipe pile; OEPP: open-ended pipe pile; CBPP: conical base pipe pile; SOEP: square open-ended pile; SCEP: square closed-ended pile and TP: tapered pile

Table 5 The ultimate compressive capacities of jacked piles

Relative density	Ultimate compressive capacity, $Q_{ult.}$ (N)											
	Pile length to diameter (L/D) ratio = 10						Ultimate compressive capacity, $Q_{ult.}$ (N)					
	CEPP	OEPP	CBPP	SCEP	SOEP	TP	CEPP	OEPP	CBPP	SCEP	SOEP	TP
Medium dense sand $D_r = 60\%$	553	385	439	518	493	566	678	453	486	610	510	704
Dense sand $D_r = 80\%$	637	425	494	594	542	670	1035	698	954	812	746	1111

CEPP: closed-ended pipe pile; OEPP: open-ended pipe pile; CBPP: conical base pipe pile; SOEP: square open-ended pile; SCEP: square closed-ended pile and TP: tapered pile

37%) comparing with that of open-ended pipe piles in the two cases of medium dense and dense sand, respectively.

In trend of tapering degree for jacked piles, it is found that the values of ultimate capacity ($Q_{ult.}$) for tapered piles with L/D of 10 and 30 in medium dense sand were found to be increased by (9% and 15%) and (15% and 38%) compared with that of square closed-ended and square open-ended piles, respectively. Also, these values were found to be increased (13% and 24%) and (37% and 49%) in the case of dense sand. These results are confirmed that the tapered piles installed in sand using jacked technique have more resistance compared with the square closed-ended piles as described by Wei [40] and Wei and El-Naggar [41]. This observation is due to the tapering degree increases the effective radius of influenced zone around the pile shaft. The densification of sand surrounding pile walls is produced additional lateral pressures led to increase the shear stresses through the pile-soil surface as indicated by Manandhar and Yasufuku [24]. The results indicated that the tapering degree has a beneficial influence on the axial pile capacity.

Influence of relative sand density

Figures 8 and 9 show the influence of relative sand density (D_r) on the ultimate axial pile load. These figures give the relation between the ultimate axial load of different model piles and different relative sand densities. There are indicated that the ultimate compressive load of different model piles increases with the increase in relative sand density.

Figure 8 shows the relation between the ultimate axial load of different non-displacement piles and different relative sand densities. It is observed that for piles with L/D of 10 and 30, the ultimate load of piles in the case of dense sand were found to be increased by (11%, 68%, 33%, 15%, 42% and 29%) and (32%, 84%, 18%, 39%, 69% and 43%) compared with that of piles in medium dense sand for the six models of closed-ended pipe, open-ended pipe, conical base pipe, square closed-ended, square open-ended and tapered piles, respectively. Comparing the results shown in Fig. 8; it is found that there is a large difference between the corresponding ultimate capacities ($Q_{ult.}$). This observation is due to the mobilized lateral earth pressure coefficient K along the pile shaft increases with the increases of sand relative density as reported by Han et al. [17].

Furthermore, Fig. 9 shows the relation between the ultimate load of different jacked piles and different sand relative densities. This figure indicates that for piles with L/D of 10 and 30, the ultimate load of piles in the case of dense sand were found to be increased by (15%, 11%, 13%, 15%, 10% and 18%) and (53%, 54%, 96%, 33%, 46% and 58%) compared with that of piles in medium dense sand for the six models of closed-ended pipe, open-ended pipe, conical base pipe, square closed-ended, square open-ended and tapered piles, respectively. This figure also confirmed that the particle crushing in dense sand is more intense than in medium-dense sand as described by Tovar-Valencia et al. [38]. It is mentioned that the relative sand density is the most effective factor on the pile capacity.

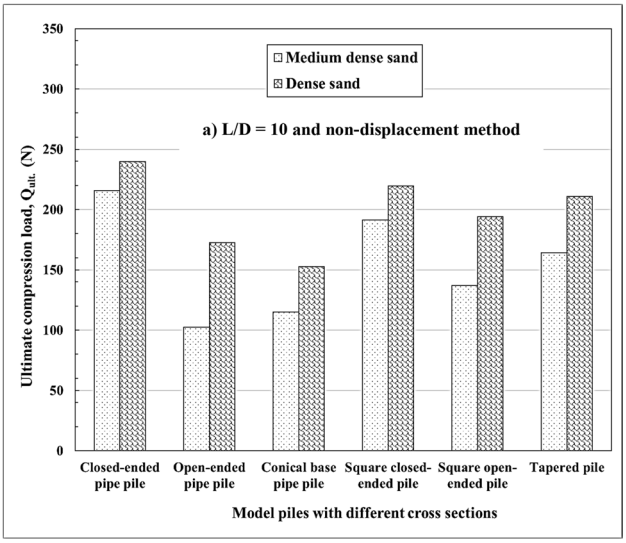

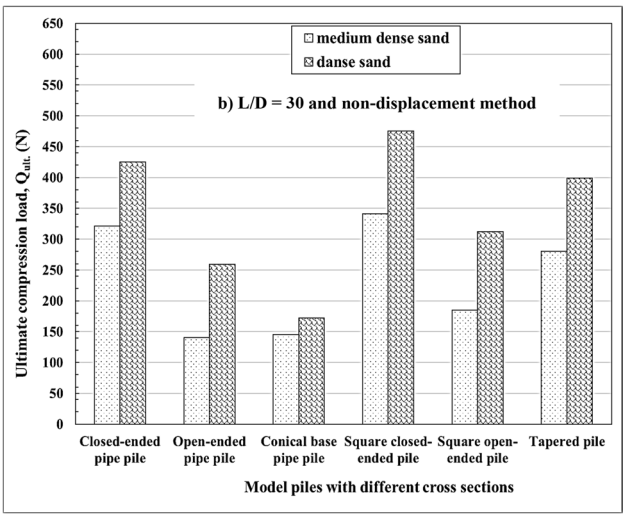

Fig. 8 Variation of compression load of different non-displacement piles with varied sand relative density

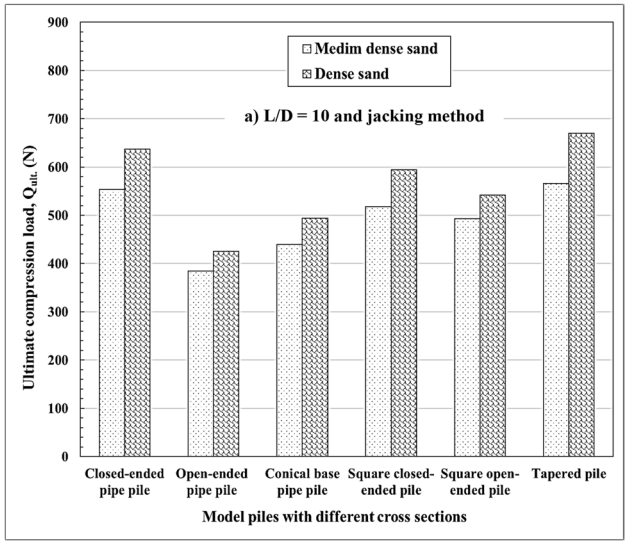

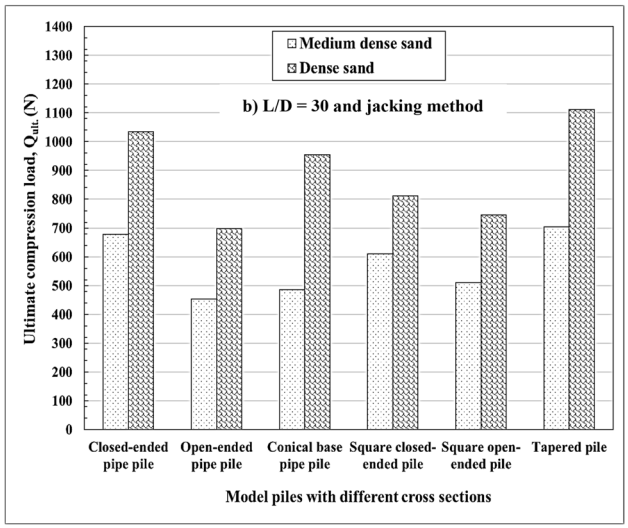

Fig. 9 Variation of compression load of different jacked piles with varied sand relative density

Influence of (pile length/diameter) ratio

The effect of (pile length/diameter) ratio, L/D on the ultimate load for different model piles, is studied and presented in Figs. 10, 11, 12 and 13. These figures indicate the relation of the ultimate load for model piles with different (pile length/diameter) ratio. These figures indicated that the pile capacity increases with the increase in the (pile length/diameter) ratio. This observation due to higher shaft resistance from larger surface area. It is clearly indicated that the compression pile capacity is highly affected by the pile length to diameter ratio.

Figures 10, 11 show the relation between the ultimate load of different non-displacement piles with different pile length/diameter ratio for the two cases of medium dense and dense sand, respectively. These figures indicate that the ultimate compressive capacities of closed-ended pipe piles with $L/D = 30$ were found to be increased by 49% and 77% compared with that of piles with $L/D = 10$ for the two cases of medium sand and dense sand, respectively, while these values for piles with the same diameter were found to be increased by (37% and 50%) and (26% and 13%) for open-ended and conical base pipe piles, respectively. From the analyzed results among piles having the same diameter, it is found that there is a difference in the increases of ultimate compressive capacities between the closed-ended and open-ended pipe piles. This observation may be due to that the closed-ended pipe piles have a large cross-sectional area.

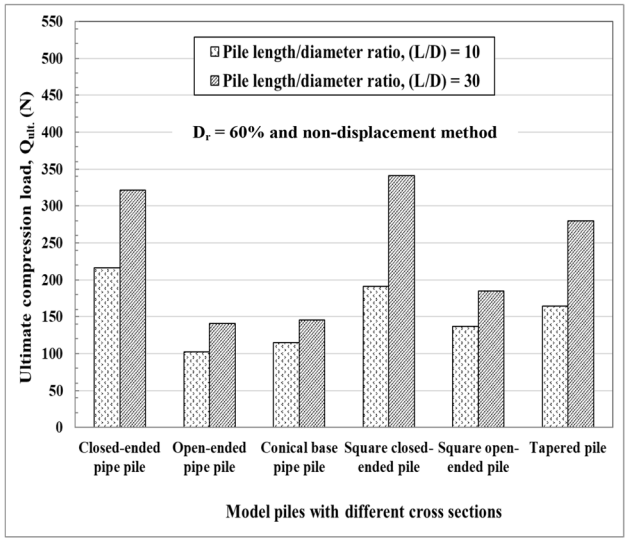

Fig. 10 Compressive load of different piles with different pile length/diameter (*L*/*D*) ratios (D_r = 60% and non-displacement technique)

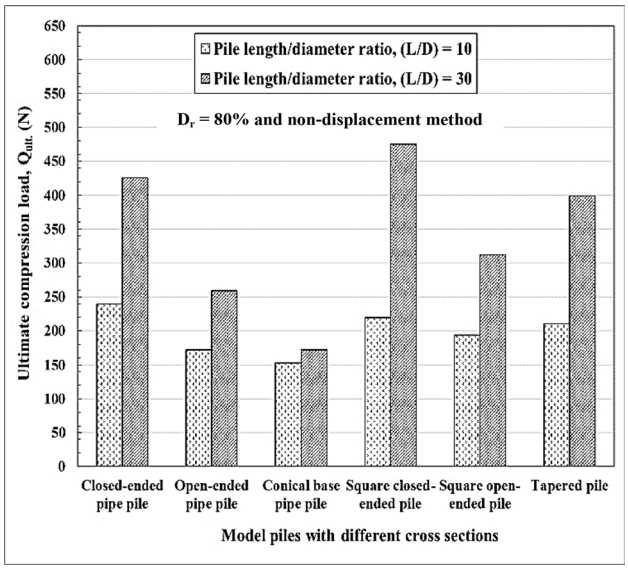

Fig. 11 Compressive load of different piles with different pile length/diameter (*L*/*D*) ratios (D_r = 80% and non-displacement technique)

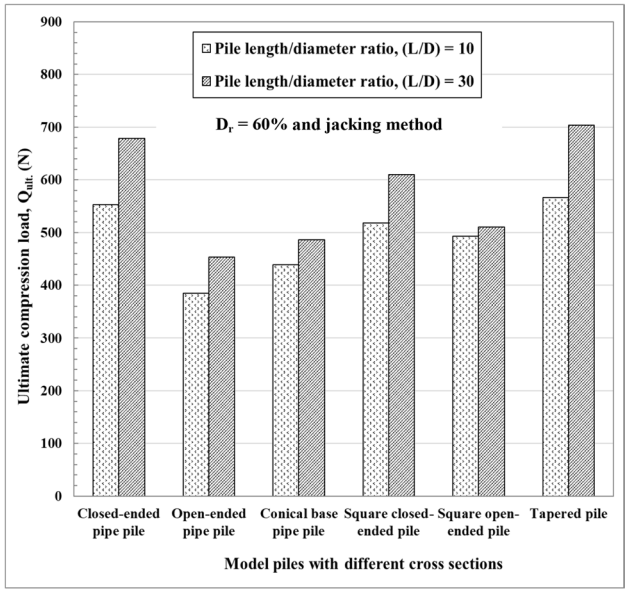

Fig. 12 Compressive load of different piles with different pile length/diameter (*L*/*D*) ratios (D_r = 60% and jacking technique)

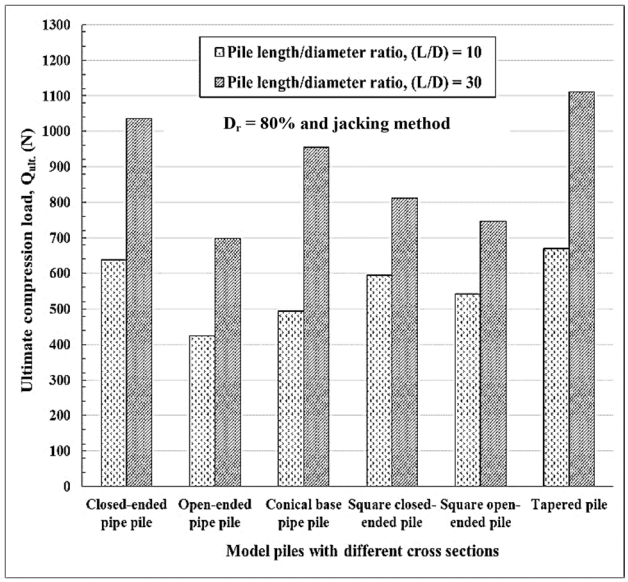

Fig. 13 Compressive load of different piles with different pile length/diameter (*L*/*D*) ratios (D_r = 80% and jacking technique)

Also, Fig. 10 indicates the response of compressive capacities for open-ended pipe piles are slightly increased with the variation of L/D ratio from 10 to 30 in the case of medium dense sand. This observation due to the formations of medium dense sand that have small void ratios and round particles. Therefore, a large energy of the pile resistance during the process of compressive loading is lost to rearrange the sand particles that surrounding pile's wall and underneath the pile tip as well as mobilized the sand soil inside the open ends of pile (Yuan et al. [43]).

These figures also indicate that the compressive capacities of square closed-ended piles with *L*/*D* = 30 were found to be increased by 78% and 116% compared with that of

piles with $L/D = 10$ for the two cases of medium sand and dense sand, respectively, while these values for piles with the same width were found to be increased by (35% and 61%) and (71% and 89%) for square open-ended and tapered piles, respectively.

On the other hand, Figs. 12 and 13 show the relation between the ultimate load of different jacked piles with different (pile length/diameter) ratio for the cases of medium dense and dense sand, respectively. These figures indicate that the ultimate compressive capacities of closed-ended pipe piles with $L/D = 30$ were found to be increased by 23% and 62% compared with that of piles with $L/D = 10$ for the cases of medium sand and dense sand, respectively, while these values for piles with the same diameter were found to be increased by (18% and 64%) and (11% and 93%) for open-ended and conical base pipe piles, respectively.

From the findings among piles having the same diameter; it is found that the difference in the increases of compressive capacities between pipe piles seemed a slight difference. These figures also show that the compressive capacities of square closed-ended piles with $L/D = 30$ were found to be increased by 18% and 37% compared with that of piles with $L/D = 10$ for the cases of medium sand and dense sand, respectively, while these values for piles with the same width were found to be increased by (4% and 38%) and (24% and 66%) and (214%, 30% and 65%) for square open-ended and tapered piles, respectively. From the results among piles having the same width; it is found that the increases in the compressive capacities of the tapered piles are being highly values due to the effect of tapering degree for tapered piles.

Furthermore, Fig. 12 indicates the increase in compressive capacity for square open-ended piles is so small with the increase in L/D ratio from 10 to 30 in the case of medium dense sand. This observation due to that the square shape helps the sand grains surrounding the pile's walls and underneath the pile tip to smoothly displace inside its open ends during the process of installation technique. Therefore, significant random changes in the void ratio and stress state of the soil mass occurred during the process of jacking installation technique as described by Basu and Prezzi [6]. Hence, the shaft resistance of square open-ended pile reduced due to the soil disturbance surrounding the outer pile's walls. So, for square open-ended pile, the measurements of compressive loads are decreased with the increase in vertical displacement readings.

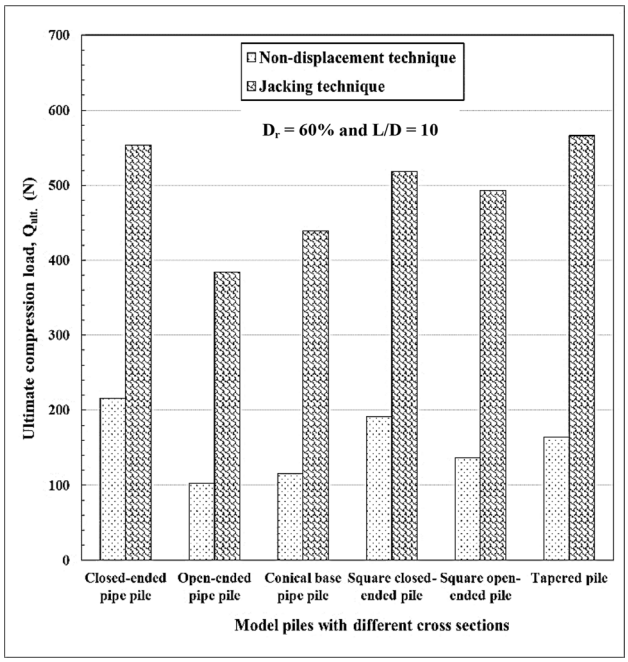

Fig. 14 Compressive load of different piles with different pile installation techniques ($D_r = 60\%$ and $L/D = 10$)

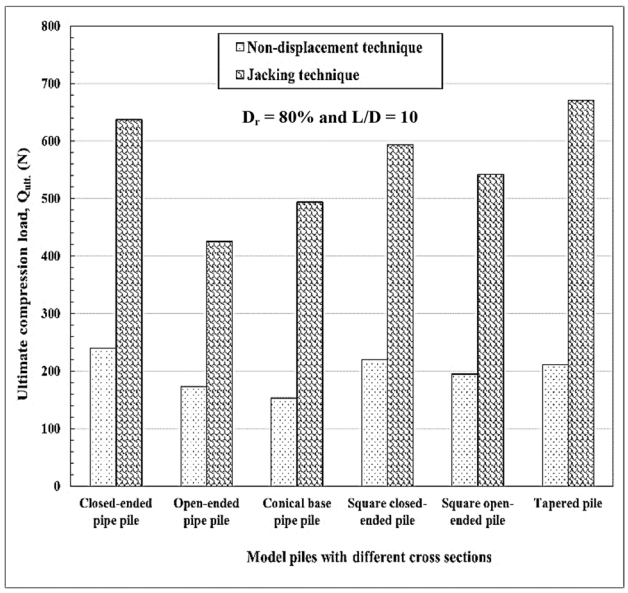

Fig. 15 Compressive load of different piles with different pile installation techniques ($D_r = 80\%$ and $L/D = 10$)

Influence of pile installation technique

In order to study the influence of pile installation technique on the compressive capacities for model piles with different cross-section geometries, Figs. 12, 13, 14, 15, 16 and 17 are shown. These figures indicate the relation between the ultimate compressive capacities for piles with different cross-section geometries and different pile installation technique methods. These figures indicated that the jacked piles have

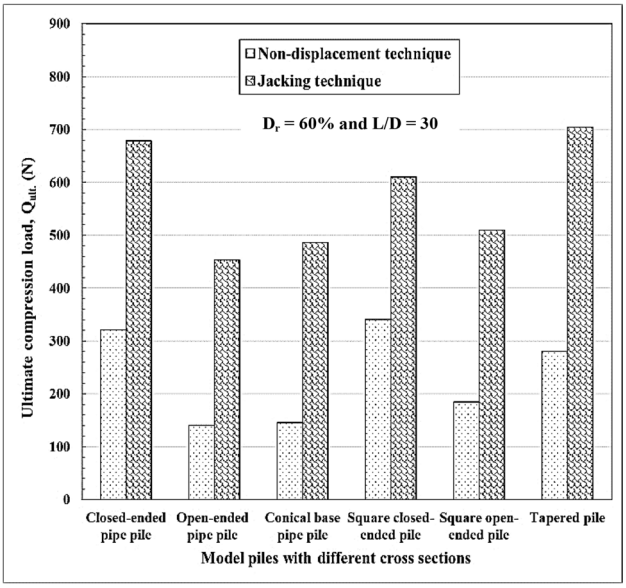

Fig. 16 Compressive load of different piles with different pile installation techniques (D_r = 60% and L/D = 30)

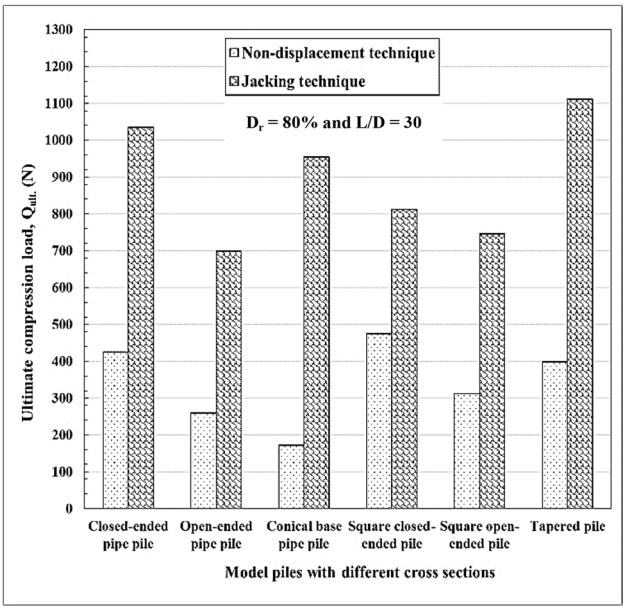

Fig. 17 Compressive load of different piles with different pile installation techniques (D_r = 80% and L/D = 30)

more resistance compared with non-displacement piles. Figures 14 and 15 indicate the relation between the compressive capacities of model piles with L/D = 10 and the different pile installation techniques for the two cases of medium dense and dense sand, respectively. On the other hand, Figs. 16 and 17 indicate the relation between the compressive capacities of model piles with L/D = 30 and the different pile installation techniques for the two cases of medium dense and dense sand, respectively.

It should be noted that the response of non-displacement piles differs from that of jacked piles due to the large densification of the sand soil during the jacked installation technique [6–41]. On the other hand, the response of compressive pile capacity is highly depending on the cross-section geometries and the used method of pile installation techniques [19]. Based on that it should be focused on the difference between pile cross-section geometries in the same pile installation technique.

Non-displacement piles

The summary of the compressive capacities for non-displacement piles is presented in Table 4. For piles with the same diameter, in the case of L/D = 10, the compressive capacities of closed-ended pipe piles were found to be increased by (110% and 87%) and (39% and 57%) compared with that of open-ended pipe piles and conical base pipe piles in the two cases of medium dense and dense sand, respectively, while, for piles with L/D = 30, the compressive capacities of closed-ended pipe piles were found to be increased by 128% and 64% compared with that of open-ended pipe piles in the cases of medium dense and dense sand, respectively. Moreover, for piles with 30, the compressive capacities of closed-ended pipe piles were found to be increased by 121% and 147% compare with that of conical base pipe piles in the cases of medium dense and dense sand, respectively. Moreover, for the two cases of L/D = 10 and 30, the compressive capacities of conical base pipe piles were found to be increased by (12% and 3%) compared with that of open-ended pipe piles in medium dense sand, respectively. But, in the case of dense sand, the compressive capacity of open-ended pipe pile was found to be increased by 13% and 51% compared with that of conical base pipe pile for the two cases of L/D = 10 and 30, respectively. It is clearly noted that the performance of open-ended pipe piles is higher than conical base pipe piles in the case of dense sand. This observation due to the effect of soil plugging inside the open-ends of piles increases with the increase in sand relative density [16–30].

On the other hand, for piles having the same width, in the case of L/D = 10, the compressive capacities of square closed-ended piles were found to be increased by (40% and 17%) and (13% and 4%) compared with that of square open-ended and tapered piles in the cases of medium dense and dense sand, respectively, while these values in the case of L/D = 30 were found to be increased by (84% and 22%) and (52% and 19%). In addition, for the two cases of L/D = 10

and 30, the compressive capacities of tapered piles were found to be increased by (20% and 51%) and (9% and 28%) compared with that of square open-ended piles for the two cases of medium dense and dense sand, respectively.

Jacked piles

The summary of the compressive capacities for jacked piles are introduced in Table 5. For piles with the same diameter, for the two cases of $L/D = 10$ and 30, the compressive capacities of closed-ended pipe piles were found to be increased by (44% and 50%) and (50% and 48%) compared with that of open-ended pipe piles in the cases of medium dense and dense sand, respectively. From the same table, for piles with L/D of 10 and 30, the compressive capacities of closed-ended pipe piles were found to be increased by (26% and 40%) and (29% and 8%) compared with that of conical base pipe piles in the cases of medium dense and dense sand, respectively. Also, for piles with L/D of 10 and 30, the compressive capacities of conical base pipe piles were found to be increased by (14% and 7%) and (16% and 37%) compared with that of open-ended pipe piles in the cases of medium dense and dense sand, respectively. Moreover, from Fig. 17 (in the case of dense sand), it is found that the compressive capacity of jacked conical base pipe pile is a highly increased by 455% compared with that of non-displacement pile. This observation approved that the conical base with sixty-degree configuration is the preferred end closure for open-ended pipe piles to install piles in heavy or hard layers as proposed by Associated Pile and Fitting Company [4]. In the case of piles with the same width, it is found that the compressive capacities of tapered piles with L/D of 10 and 30 in medium dense sand were found to be increased by (9% and 15%) and (15% and 38%) compared with that of square closed-ended and square open-ended piles, respectively. Also, these values were found to be increased by (13% and 24%) and (37% and 49%) in the case of dense sand.

Conclusion

Based on the present investigation for studying the effect of varied cross-section geometries on the compressive pile capacity in sand, the following conclusions can be drawn as follows:

1. Pile cross-section geometry has a significant influence on the compressive pile capacity.
2. Compressive pile capacity is highly affected by the pile length to diameter ratio. For examples, the increase in the compressive capacity for jacked square open-ended piles is so small with the increase in L/D ratio from 10 to 30 in the case of medium dense sand.
3. Out of all the compared parameters, the increase in sand relative density is the most effective on the increasing compressive pile capacity. It is demonstrated that due to improving sand relative density from medium dens state to dense state, the corresponding increases in compressive capacities are within the range of (11%–84%) and (10%–96%) for non-displacement and jacked piles, respectively.
4. In jacked piles, the tapering degree has a beneficial influence on the compressive pile capacity. Also, the tapering degree highly affected the increase in compressive capacities within the range of (9%-39%) for the two cases of medium dense and dense sand.
5. The load capacity of open-ended piles is greatly influenced by the degree of plugging soil. For example, in the case of dense sand, the compressive capacity of non-displacement open-ended pipe pile was found to be increased by 13% and 51% comparing with that of conical base pipe pile having L/D of 10 and 30, respectively.
6. Moreover, for non-displacement piles with $L/D = 10$, the compressive capacities of conical base pipe piles were found to be increased by 12% compared with that of open-ended pipe piles in medium dense sand, respectively, while, in dense sand, the compressive capacity of open-ended pipe pile was found to be increased by 13% compared with that of conical base pipe pile.
7. For non-displacement piles with the same width, the square closed-ended pile is a highly effective and having more resistance compared with the square open-ended and tapered piles.
8. The compressive capacities of jacked tapered piles with L/D of 10 and 30 in medium dense sand were found to be increased by (9% and 15%) and (15% and 38%) compared with that of jacked square closed-ended and square open-ended piles, respectively. Also, these values increased by (13% and 24%) and (37% and 49%) in the case of dense sand.
9. The conical base with sixty-degree configuration is the preferred end closure for open-ended pipe piles to provide high performance in the installation process and to achieve load capacity.

Appendix 1

See Table 6.

Table 6 Laboratory-scale studies of the effects of the pile cross-section geometry in sand

Pervious topic	Fattah and Al-Soudani [14, 15]	Jebur et al. [21]	Salih et al. [36]	Dario-Tovar et al. [9]
Research approach	Experimental	Experimental and numerical using ANN depended on LM method	Experimental	Experimental
Test tank	750 × 750 mm in plan and H_t = 750 mm	900 × 900 mm in plan and H_t = 1250 mm	D_t = 350 mm and H_t = 450 mm	D_t = 1200 mm and H_t = 1680 mm
Model pile properties	Steel open-ended pipe piles modified with closing the pile ends by a welded-plate at distance of 2D, 3D and 4D from the pile tip	D /or B = 40.0 mm and L/D = 12, 17 and 25	Steel piles with the same cross-section area of the pile tip (78.0 mm^2) and with L = 100, 150 and 200 mm	Steel piles with D = 31.75 mm and L = 915.00 mm
Pile cross-section geometry	Open-ended and closed-ended pipe piles	Square concrete, steel open-ended pipe and closed-ended pipe piles	Closed-ended pipe pile, open-ended pipe pile and H-pile	Pipe pile with a flat base and with a conical cross-sectional base with a sixty-degree configuration
Sand preparing	Raining technique	Compaction method	Compaction method	Raining technique
Sand relative density	Medium and dense sand	Dense sand (D_r = 85%)	D_r = 15%, 50% and 85% corresponding to loose, medium and dense sand	Medium and dense sand
Pile installation method	Driven and pressed	Non-displacement	Vertically driven	Jacked (displacement) and preinstalled (non-displacement)
Applied load	Axial compression load	Axial compression load	Static compression load	Static compression load

Pervious topic	Sakr et al. [34]	Manandhar et al. [26]	Manandhar and Yasufuku [27]
Research approach	Experimental	Experimental	Experimental and theoretical
Test tank	800 × 800 mm in plan and H_t = 800 mm	D_t = 750 mm and H_t = 1000 mm	D_t = 750 mm and H_t = 1000 mm
Model pile properties	Steel pipe piles, D = 20 mm, L = 200 and 600 mm and L/D = 10 and 30	1. For tapered pile T_1, D_{head} = 35 mm, D_{tip} = 25 mm and α = 0.7	1. For tapered pile T_1, D_{head} = 35 mm, D_{tip} = 25 mm and α = 0.7
		2. For tapered pile T_2, D_{head} = 45 mm, D_{tip} = 25 mm and α = 1.4	2. For tapered pile T_2, D_{head} = 45 mm, D_{tip} = 25 mm and α = 1.4
		3. For cylindrical pile, D = 25 mm	3. For cylindrical pile, D = 25 mm
		4. For all piles, L = 500 mm	4. For all piles, L = 500 mm
Pile cross-section geometry	Open-ended, closed-ended and conical base pipe piles	Tapered and cylindrical piles	Tapered and cylindrical piles
Sand preparing	Predetermined weight technique	Raining technique	Raining technique
Sand relative density	D_r = 33%, 60% and 80% corresponding to loose, medium dense and dense sand	D_r = 60% and 80% corresponding to medium and dense sand	Dense sand (D_r = 80%)
Pile installation method	Jacking	Vertically driven and cast-in-place	Cast-in-place
Applied load	Axial compression load	Compression load with constant rate of 5 mm/mim	Compression load with constant rate

D: pile diameter; B: pile width; L: pile length L/D: pile length to diameter ratio; H_t: height of test tank; D_t: diameter of test tank; D_{head}: pile head diameter; D_{tip}: pile tip diameter; α: tapering degree; D_r: sand relative density; ANN: artificial neural networks and LM: Levenberg–Marquardt method

Acknowledgements The experiments were carried out in the Geotechnical Laboratory of Structural Engineering Department, Tanta University which is acknowledges.

Declarations

Conflict of interest On behalf of all authors, the corresponding author states that there is no conflict of interest.

Ethical approval This article does not contains any studies with human participation or animals performed by any of the authors.

Informed consent For this type of study formal consent is not valid and required.

References

1. Adejumo TW (2015) Effects of shape and technology of installation on the bearing capacity of pile foundations in layered soil. Scholars J Eng Technol 3(2A):104–111
2. American Petroleum Institute (ANSI/API - Recommended Practice). (2011). Geotechnical and Foundation Design Considerations. ISO 19901–4:2003
3. American Petroleum Institute (2007) API recommended practice for planning, designing and constructing fixed offshore platforms - working stress design - RP 2A. API Publishing Services, Washington
4. Associated Pile and Fitting Company. APF-General Brochure-1017. (n.d.). Retrieved from www.associatedpile.com. Retrieved from http://www.associatedpile.com/File%20Library/Document%20Library/English/Brochures/APF_General_Brochure_1017.pdf
5. Balachowski L (2006) Scale effect in shaft friction from the direct shear interface tests. Archiv Civil Mech Eng J VI(3):14–29
6. Basu P, Prezzi M (2009) Design and applications of drilled displacement (screw) piles. Purdue University, West Lafayette, Indiana: Final Report: FHWA/IN/JTRP- 2009/28, Prepared in Cooperation with the Indiana Department of Transportation and The U.S. Department of Transportation, Federal Highway Administration
7. Basu P, Loukidis D, Prezzi M, Salgado R (2011) Analysis of shaft resistance of jacked piles in sands. Int J Numer Anal Methods Geomech 35:1605–1635
8. Bolton MD, Gui MW, Garnier J, Corte JF, Bagge G, Laue J, Renzi R (1999) Centrifuge cone penetration tests in sand. Geotechnique 49(4):543–552
9. Dario-Tovar RD, Galvis AG, Salgado R, Prezzi M (2021) Effect of base geometry on the resistance of model piles in sand. J Geotech Geoenviron Eng 147(3):1–15
10. Das, B.M. (2014). Chapter 9: Pile foundations. In Principles of foundation engineering, Eighth Edition (Pp: 391–504). United State of America: Global Engineering; Nelson Education.
11. De Beer EE (1963) The scale effect in the transposition of the results of deep-sounding tests on the ultimate bearing capacity of piles and caisson foundations. Geotechnique 13(1):39–75
12. Dharmatti V, Rakaraddi PG (2014) An experimental study on vertically loaded diven and cast-In-situ piles. J Mech Civil Eng 11(2):43–48
13. Erhart J (2016) Conical Points for ERW Pipe Piles. Retrieved from Retrieved from Atlas Observer: https://www.atlastube.com/atlas-observer/conical-points-for-erw-pipe-piles/
14. Fattah MY, Al-Soudani WHS (2015) Bearing capacity of open-ended pipe piles with restricted soil plug. Ships Offshore Struct, pp 1–16
15. Fattah MY, Al-Soudani WHS (2016) Bearing capacity of closed and open ended pipe piles installed in loose sand with emphasis on soil plug. Indian J Geo-Marine Sci 45(5):703–724
16. Garnier J, Gaudin C, Springman SM, Culligan PJ, Goodings D, Konig D, Kutter B, Phillips R, Randolph MF, Thorel L (2007) Catalogue of scaling laws and similitude questions in geotechnical centrifuge modelling. Int J Phys Modell Geotech 3:1–23
17. Han F, Salgado R, Prezzi M, Lim J (2017) Shaft and base resistance of non-displacement piles in sand. Comput Geotech 83:184–197
18. Henke S (2020) Soil plug investigation with respect to pile geometry and installation method. In: Laue JA (ed) 4th European conference on physical modelling in geotechniques. Lulea University of Technology, Sweden, pp 25–132
19. Ibrahim SF, Al-Soud MS, Al-Asadi FI (2018) Performance of a single pile under combined axial and lateral loads in layered sandy soil. J Eng Sustain Dev 22(1):121–136
20. Jardine RJ, Chow FC (2007) Some recent development in offshore pile design. In: 6th of Offshore Site Investigation Geotechnics Conference. London
21. Jebur, A.A., Atherton, W., Alkhadar, R.M. and Loffill, E. (2017). Piles in sandy soil: a numerical study and experimental validation. Procedia Engineering Journal, 196, Pp: 60–67.
22. Jeong DI, Kim YO (2005) Rainfall-runoff models using artificial neural networks for ensemble stream flow prediction. Hydrol Process 19(19):3819–35
23. Klotz U (2000) The influence of state on the capacity of driven piles in sands. Ph. D. Thesis submitted to City University. London
24. Kraft LM (1991) Performance of axially loaded pipe pile in sand. J Geotech Eng 117(2):272–296
25. Liew SS, Ho SF (2016) Fallacy of capacity performance & innovation improvement of jack-in piling in Malaysia. Geotech Eng J SEAGS & AGSSEA 47(4):134–144
26. Manandhar S, Yasufuku N, Omine K, Kobayashi T (2010) Response of tapered piles in cohesionless soil based on model tests. J Nepal Geological Soc 40:85–92
27. Manandhara S, Yasufukub N (2013) Vertical bearing capacity of tapered piles in sands using cavity expansion theory. Soils Found J Jpn Geotech Soc 53(6):853–867
28. Meyerhof GG (1976) Bearing capacity and settlement of pile foundations. J Geotech Eng Division Am Soc Civil Eng 102(GT3):197–228
29. Nazir A, Nasr A (2013) Pullout capacity of batter pile in sand. J Adv Res Cairo Univ 4:147–154
30. Paik K, Salgado R, Lee J, Kim B (2003) Behavior of open- and closed-ended piles driven into sands. J Geotech Geoenviron Eng 129(4):296–306
31. Phillips R, Valsangkar AJ (1987) An experimental investigation of factors affecting penetration resistance in granular soils in centrifuge modeling. Department of Engineering, Cambridge University, England: Report CUED/D-Soils TR 210
32. Rahil FH, Al-Neami MA, Al-Zaho KAN (2016) Effect of relative density on behavior of single pile and piles groups embedded with different lengths in sand. Eng Technol J 34(6):1206–1216
33. Robinsky EI, Morrison CF (1964) Sand displacement and compaction around model friction piles. Can Geotech J 1(2):81–93
34. Sakr MA, Azzam WR, Kassim HK (2021) Model study of jacked pile with varied geometry in sand. International Conference on Advances in Structural and Geotechnical Engineering (ICASGE'21). Hurghada: Faculty of Engineering, Tanta University, Egypt pp 1–13

35. Salem TN, Elkhawas NM, Elnady AM (2021) Behavior of offshore pile in calcareous sand-case study. J Marine Sci Eng 9(839):1–18
36. Salih SJH, Salih NB, Noory DB (2020) Optimum design of steel piles in different sandy soil configurations. Int J Geomech Geoeng, pp 1–22
37. Terzaghi K (1943) Theoretical soil mechanics. Wiley, New York
38. Tovar-Valencia DD, Galvis-Castro A, Salgado R, Prezzi M, Fridman D (2022) Experimental measurement of particle crushing around model piles. Acta Geotech, Pp: 1–21
39. Wei J (1998) Experimental investigation of tapered piles. Master Degree Thesis submitted to The University of Western Ontario, National Library of Canada. London
40. Wei J, El Naggar MH (1998) Experimental study of axial behaviour of tapered piles. Can Geotech J 36(6):1204–1205
41. White DJ, Deeks AD (2007) Recent research into the behaviour of jacked foundation piles. Proceedings of the international workshop on recent advances in deep foundations. Yokosuka, Japan: Reaserch Gate pp 1–23
42. Yang J, Tham LG, Lee PKK, Chan ST, Yu F (2006) Behaviour of jacked and driven piles in sandy soil. Geotechnique 56(4):245–259
43. Yuan B, Chen R, Teng J, Wang Y, Chen W, Peng T (2015) Effect of sand relative density on response of a laterally loaded pile and sand deformation. Hindawi Publishing Corporation. J Chem 2015:1–6